Atmos. Meas. Tech. Discuss., 6, 6187–6213, 2013
www.atmos-meas-tech-discuss.net/6/6187/2013/
doi:10.5194/amtd-6-6187-2013

Atmospheric Measurement Techniques Discussions
Open Access

Validation of FORMOSAT-3/COSMIC level 2 "atmPrf" global temperature data in the stratosphere

U. Das and C. J. Pan

Institute of Space Science, National Central University, Jhongli 32001, Taiwan

Received: 5 May 2013 – Accepted: 1 July 2013 – Published: 9 July 2013

Correspondence to: C. J. Pan (cjpan@jupiter.ss.ncu.edu.tw)

Published by Copernicus Publications on behalf of the European Geosciences Union.

Abstract

GPS radio occultations by Formosa Satellite mission-3/Constellation Observing System for Meteorology, Ionosphere, and Climate (FORMOSAT-3/COSMIC) provide refractivity profiles, which are processed real-time to give profiles of temperature and water vapour in the lower atmosphere and electron density in the upper atmosphere. The new "atmPrf" (atmospheric profile) product gives temperature from surface to 0.2 hPa (∼ 60 km). This is a dry temperature data product that does not include relative humidity in the inversion process and hence is reliable at and above the tropopause (> 100 hPa) and erroneous in the troposphere (< 100 hPa). In the current study we compare the COSMIC "atmPrf" data during December 2010 to November 2011 with other satellite (SABER/TIMED and MLS/Aura) temperatures from 50 to 0.2 hPa and reanalysis (NCEP, ERA-Interim and UKMO) outputs at 100, 10, 1 and 0.5 hPa pressure levels. The satellite comparisons show that the observed median differences are most likely produced due to the biases in the retrievals of SABER and MLS. When compared to reanalysis outputs, COSMIC seasonal means match NCEP and ECMWF seasonal mean temperatures very well, especially at 100 and 10 hPa. Comparison with radiosonde measured temperatures over Taipei (25° N, 121.5° E) in the lower altitudes also show very small differences. We conclude from this study that with the new COSMIC dry temperature retrievals obtained from radio occultations of GPS, there is a 20 km extension of reliable data in the middle atmosphere. "atmPrf" data are of good quality and provide reliable and unprecedentedly large number of profiles at greater temporal and spatial resolutions for further studies and investigations of the middle atmosphere up to 1 hPa, i.e., approximately up to the stratopause.

1 Introduction

Understanding the thermal structure of the lower and middle atmosphere is very important to understand the system and its dynamics. This knowledge is very important

AMTD
6, 6187–6213, 2013

for climate change studies, troposphere–stratosphere and stratosphere–troposphere exchange processes, coupling of lower to upper atmosphere, and vice versa, etc. Temperature measurements had been made from various ground-, rocket-, balloon- and satellite-based platforms over the last few decades. Ground-based measurements by lidars (for e.g., Hauchecorne and Chanin, 1980), provide very good accuracy but are present only over a few locations over land. Similarly, rocket (for e.g., Clark and McCoy, 1965) and balloon (for e.g., Rinsland et al., 1983) observations are also very sparse in space and time, although they provide the most accurate measurements. In addition, experiments from these platforms are very expensive. With the satellite era growing, observations from space (Dessler et al., 1998) are presenting a more global view and providing continuous measurements over all latitudes and longitudes.

Satellite temperature retrievals from atmospheric refractivity measurements using state-of-the-art technique, Global Positioning System based Radio Occultation (GPS RO) soundings, have provided the research community with a wealth of data to investigate the lower and upper atmosphere (Wickert et al., 2001, 2005). Comparisons with radiosonde measurements revealed that RO is a robust measurement technique for atmospheric monitoring and is sufficiently accurate to differentiate the variation in performance among various types of radiosonde (Kuo et al., 2005). The Formosa Satellite mission 3/Constellation Observing System for Meteorology, Ionosphere, and Climate (FORMOSAT-3/COSMIC) has further moved a step ahead providing temperature data with unprecedentedly large number of measurements using this technique (Anthes et al., 2008; Fong et al., 2009). COSMIC measurements provide global coverage, high spatial, vertical and temporal resolutions, long-term stability, self-calibration and capability to operate in all weather conditions. The inversion and error estimations of GPS RO data are discussed in detail by Kuo et al. (2004).

Earlier Kishore et al. (2009) validated the COSMIC “wetPrf” temperatures with reanalysis outputs of National Centers for Environmental Prediction (NCEP), UK Met Office (UKMO), and Japanese 25 yr Reanalysis (JRA-25) in the altitude region from 8 to 30 km, with emphasis on the 100 hPa pressure level. They found that the COS-

MIC temperatures best resembled the NCEP temperatures. Similar assessment was made with Vaisala-RS92 and Shanghai radiosonde temperatures and close-to-zero mean differences were observed in the troposphere and lower stratosphere (He et al., 2009). In the current study, we are validating a new dataset called the "atmPrf", i.e., atmospheric profile, which gives temperature to much higher altitudes up to the lower mesosphere (60 km). However, this is a dry temperature data product that does not include relative humidity in the inversion process and hence is erroneous in the troposphere. We thus concentrate on altitudes from the tropopause to the lower mesosphere from 100 to 0.2 hPa. In this study we compare the COSMIC "atmPrf" temperature data from December 2010 to November 2011 with temperatures measured by Sounding of the Atmosphere using Broadband Emission Radiometry (SABER) instrument on board the Thermosphere–Ionosphere–Mesosphere Energetics and Dynamics (TIMED) satellite and Microwave Limb Sounder (MLS) instrument on board Aura satellite from 50 to 0.2 hPa and with reanalysis outputs of NCEP, ECMWF (European Centre For Medium-Range Weather Forecasts) Interim Reanalysis (ERA-Interim), and UKMO at 100, 10, 1 and 0.5 hPa pressure levels on the seasonal scale. We also compare with the radiosonde measurements over Taipei (25° N, 121.5° E) near the tropopause and in the lower stratosphere. We show that COSMIC "atmPrf" temperatures are of good quality and provide unprecedentedly large number of observations to further the studies and investigations of the middle atmosphere up to the stratopause region (∼ 50 km) that were not possible earlier as reliable temperature data was available only up to ∼ 30 km.

2 Data and analysis

2.1 FORMOSAT-3/COSMIC temperature data

The FORMOSAT-3/COSMIC mission comprises of a constellation of six micro satellites that were launched into a circular, 72° inclination orbit at an altitude of 512 km on 15

April 2006. The mission goal was to deploy the six satellites into six orbit planes at 800 km with a 30° separation for evenly distributed global coverage, which has been successfully achieved. It is the first constellation of satellites for monitoring global weather and ionospheric electron density distribution using the GPS RO technique. Further details regarding the spacecraft constellation system can be obtained from Fong et al. (2009). COSMIC provides the refractivity profiles, which are processed real-time by the COSMIC Data Analysis and Archive Center (CDAAC) at the University Corporation for Atmospheric Research (UCAR) to give profiles of temperature and water vapour in the lower and middle atmosphere. The level 2 "atmPrf" data product of COSMIC provides dry temperature from surface to 60 km, by neglecting the water vapour information, and hence is suitable for the investigations of stratosphere and lower mesosphere. Details of temperature retrievals from refractivity profiles obtained from GPS RO soundings can be obtained in literature (Kursinski et al., 1997; Kuo et al., 2004; Anthes et al., 2008).

All COSMIC "atmPrf" temperature profiles during December 2010 to November 2011 are interpolated from 10 to 60 km at 0.1 km altitude spacing and 0.05 (in log scale) pressure spacing. The profiles are gridded into four-dimensional space-time coordinates, i.e., latitude (10°), longitude (10°), altitude/pressure and local time (2 h). At each point in three-dimensional space, monthly averages for every two hours are computed that are later averaged over all local times to get the monthly means. These monthly means are then utilised to obtain the seasonal means during DJF (December 2010–February 2011), MAM (March–May 2011), JJA (June–August 2011), and SON (September–November 2011).

The top row of Fig. 1 shows the global distribution of the number of COSMIC observations in space and time during the study period. Number of observations is marginally higher over the mid-latitudes around ±50° latitudes and very uniformly distributed in longitude. The observations during the day over mid-latitudes are almost twice that over the equator at midnight. From a seasonal point of view, observations are highest during MAM and JJA.

AMTD
6, 6187–6213, 2013

2.2 SABER/TIMED temperature data

The TIMED satellite was launched in December 2001 in a sun-synchronous polar orbit at 625 km with an inclination of 74.1°. The satellite makes ~ 15 orbits per day with a period of 1.6 h and takes 60 days to complete a full 24 h cycle in local time. SABER is one of the four instruments onboard the TIMED satellite whose aim is to advance the understanding of the structure, energetics, chemistry and dynamics of the atmosphere from 20 to 120 km. SABER measures the Earth limb emissions in 10 broad band radiometer channels ranging from 1.27 to 17 µm. The kinetic temperature from the tropopause to the lower thermosphere is retrieved from CO_2 15 µm limb emission using a full non-local thermal equilibrium (non-LTE) inversion method. In the present study we have used the SABER 2A level data product of version 1.07 from December 2010 to November 2011. Comparison of the latest 1.07 version temperatures with other ground-based observations show that the SABER temperatures are higher by 1 to 3 K in the lower stratosphere and slightly lower by 1 to 3 K in the upper stratosphere and lower mesosphere and concluded that the temperatures of this version are of good quality (Remsberg et al., 2008).

The middle row of Fig. 1 shows the global distribution of the number of SABER observations in space and time during the study period. Similar to the COSMIC coverage, the number of observations over mid-latitudes at ±50° latitudes is higher and very uniformly distributed in longitude. In contrast, the number of observations are practically absent during noon at all latitudes and longitudes. This is due to the orbital nature of the TIMED satellite. From the seasonal point of view, higher number of observations is present during MAM in the Northern Hemisphere and during SON in the Southern Hemisphere.

2.3 MLS/Aura temperature data

The Earth Observing System (EOS) MLS is one among the four instruments onboard the NASA's EOS Aura satellite, launched on 14 July 2004 into a 705 km near-polar or-

AMTD
6, 6187–6213, 2013
Validation of COSMIC data
U. Das and C. J. Pan

bit. As Earth rotates underneath it, the Aura orbit stays fixed relative to the sun, to give daily global coverage with ∼ 14 orbits per day and observations at fixed local time. MLS provides ∼ 3500 vertical profiles each day up to a latitude of 82° in each hemisphere (Waters et al., 2006). MLS temperature is retrieved from thermal microwave limb emission bands of O_2 at 118 GHz and 239 GHz. The isotopic 239 GHz line is the primary source of temperature information in the troposphere, while the 118 GHz line is the primary source of temperature in the stratosphere and above. In the current study we have used the version 3.3 temperature retrievals (Livesey et al., 2011) and focussed on the pressure levels from 100 to 0.1 hPa during December 2010 to November 2011. The observed bias uncertainties (in K) are 0 to +1, −1 to 0, 0 to +5, −7 to −4 and −8 to 0 at 100, 10, 1, 0.316 and 0.1 hPa and precisions of this data product are ±0.8, ±0.6, ±1, ±1 and ±2 K, respectively at the five pressure levels (Schwartz et al., 2008).

The last row of Fig. 1 shows the global distribution of the number of MLS observations in space and time during the study period. Due to the fixed orbit of the Aura satellite, number of observations is constant at all latitudes and longitudes except at around ±70° where the satellite ascends/descends. Observations are available at all latitudes and longitudes only at 1.30 a.m. and 1.30 p.m. (local time). It can be concluded from Fig. 1 that COSMIC has a more uniformly distributed global coverage, especially in local time, in comparison to SABER and MLS observations and is due to the fact that COSMIC is a constellation of six micro satellites.

2.4 Radiosonde observations

Temperatures measured using radiosonde over Banqiao, Taipei from 300 to ∼ 10 hPa during December 2010 to November 2011 are also used for comparison with the COSMIC temperatures. The data were collected by the Central Weather Bureau of Taiwan using the standard radiosonde, Vaisala RS92-SGPD. The radiosondes are flown twice every day at 00:00 and 12:00 h UTC.

AMTD
6, 6187–6213, 2013

2.5 NCEP reanalysis temperature data

The NCEP/NCAR Reanalysis project uses state-of-the-art analysis/forecast system to perform data assimilation using past data from 1948 to the present (Kalnay et al., 1996). A large subset of this data is available in its original 4 times daily format and as daily and monthly averages. The data is available at 17 pressure levels from 1000 to 10 hPa on a 2.5° latitude by 2.5° longitude global grid. In the current study, seasonal averages are obtained from monthly averages for comparison with the COSMIC data at pressure levels 100 and 10 hPa during December 2010 to November 2011.

2.6 ERA-Interim temperature data

ERA-Interim is the latest global atmospheric reanalysis produced by the ECMWF (Dee et al., 2011). The ERA-Interim project was conducted in part to prepare for a new atmospheric reanalysis to replace ERA-40, which will extend back to the early part of the twentieth century. This reanalysis data is produced with a sequential data assimilation scheme, advancing forward in time using 12 hourly analysis cycles. In each cycle, available observations are combined with prior information from a forecast model to estimate the evolving state of the global atmosphere and its underlying surface. This involves computing a variational analysis of the basic upper-air atmospheric fields (temperature, wind, humidity, ozone and surface pressure), followed by separate analyses of near surface parameters, soil moisture and soil temperature, snow and ocean waves. The analyses are then used to initialise a short-range model forecast, which provides the prior state estimates needed for the next analysis cycle. Data is available from 1979 onwards at 37 pressure levels from 1000 to 1 hPa at a spatial resolution of 1.5° × 1.5°. In the current study, seasonal averages are obtained from monthly averages at pressure levels 100, 10 and 1 hPa for comparison with the COSMIC data during December 2010 to November 2011.

AMTD
6, 6187–6213, 2013

2.7 UKMO stratospheric assimilated temperature data

UKMO provides data concerning stratospheric temperature, geopotential height and wind components produced by the Stratospheric Data Assimilation System. The data assimilation system is a development of the scheme used at the Met Office for operational weather forecasting, which has been extended to cover the stratosphere by the Middle Atmosphere Group. The primary product is a daily analysis, at 12:00 UT, which is produced using only operational observations from 17 October 1991 onwards. These data are sets of meteorological analyses at 25 pressure levels from 1000 to 0.1 hPa on a 2.5° latitude by 3.75° longitude global grid. In 2000, the data assimilation system was converted to a 3-D Variational (3-D-VAR) assimilation system that allows a statistically better combination of information from both observations and the model background (Lorenc et al., 2000; Swinbank and Office, 2002). In the current study, seasonal averages are obtained from monthly averages at pressure levels 100, 10, 1 and 0.5 hPa for comparison with the COSMIC data during December 2010 to November 2011.

2.8 Analysis

Temperature differences between COSMIC and SABER, and COSMIC and MLS are investigated using near-simultaneous measurements within ±5° latitude by ±5° longitude and one hour local time. These differences are grouped into different latitude regions (−80° to −50°, −50° to −20°, −20° to 20°, 20° to 50°, 50° to 80°) and seasons (DJF, MAM, JJA, SON) and a statistical investigation is carried out by comparing the medians and their standard deviations.

To compare COSMIC temperatures, which are gridded at a coarser spatial resolution, with those of NCEP, ERA and UKMO, the reanalysis seasonal means are undersampled to match the latitude and longitude grid spacing of COSMIC means. Global comparisons are made at 100, 10, 1 and 0.5 hPa pressure levels. NCEP data are available only at 100 and 10 hPa, ERA at 100, 10 and 1 hPa and UKMO at all the four pressure levels of interest. The comparisons are made accordingly, by investigating

AMTD
6, 6187–6213, 2013

the differences between seasonal mean temperatures of COSMIC and the different reanalysis outputs.

Finally, global mean temperature profiles from all the above listed satellites and reanalysis outputs are also compared with that of COSMIC.

3 Comparison with other satellite temperatures

The first and second columns of Fig. 2 show the seasonal median temperature differences between COSMIC and SABER temperatures obtained from near simultaneous observations in space and time and the corresponding standard deviations, respectively. Measurements within ±5° latitude and longitude and one hour local time have been chosen for the comparison. The four profiles in each panel show the differences during different seasons – DJF (black), MAM (green), JJA(red), and SON (blue) – and the different rows pertain to different latitudinal bands. No differentiation is made with respect to longitude and local time. The numbers in the left top corner are the numbers of profiles available for comparison during each season. Maximum numbers of simultaneous observations are available in the 20° to 50° and −50° to −20° latitudinal bands, as the TIMED spacecraft is moving in a sun synchronous polar orbit and provides more observations near 50° latitude during each 60 day yaw cycle.

The seasonal median temperature differences in different latitude regions show that the COSMIC temperatures are less than SABER temperatures by 2–3 K at the lower altitudes (∼ 50 hPa) and gradually increase with altitude to become higher by the same amount at 1 hPa. At higher altitudes of ∼ 0.2 hPa the differences increase further to 5–7 K and in the Southern Hemisphere high altitudes, the differences are as high as 10 K. At ∼ 3 hPa the differences are very close to zero. This pattern is very systematic in all latitude regions and during all seasons. The standard deviations over the low-latitudes are ∼ 2 K at 50 hPa, increase with altitude, are less than 5 K up to altitudes > 1 hPa and maximum deviations of 6–7 K are observed at ∼ 0.5 hPa, where after they start to decrease. This pattern is also similar during all seasons. Over mid-latitudes also the

AMTD
6, 6187–6213, 2013

standard deviations at 50 hPa are ~ 2 K except in Northern Hemisphere winter (~ 3 K) and increase with height. At 1 hPa the deviations vary from 5 to10 K and maximise (6–10 K) at ~ 0.5 hPa. In both hemispheres, summer deviations are lowest and winter deviations are highest at each pressure level. Over high-latitudes, the deviations at 50 hPa range from 2 to 4 K and maximise at ~ 0.5 hPa. Largest deviations of 15 K occur during winter, while summer deviations are almost similar to that over mid-latitudes.

Remsberg et al. (2008) compared SABER temperatures with ground-based lidar measurements and showed that the SABER temperatures are higher by 1–3 K in the lower stratosphere (below 40 km or ~ 3 hPa), similar at 40 km, and lower by 1–3 K in the upper stratosphere and lower mesosphere (40–60 km). This is due to the bias error in the CO_2 radiances of the wide channel or Ch 3 (580–763 cm^{-1}) below 40 km combined with a changeover from relying on both Ch 3 and the narrow channel or Ch 1 (649–698 cm^{-1}) radiances at 40 km to relying on just the Ch 1 radiances at 50 km for the temperature retrievals (Mertens et al., 2001; Remsberg et al., 2008). Interestingly, these biases and the systematic pattern in the median differences of COSMIC and SABER temperatures observed in the present study are very similar.

The third and fourth columns of Fig. 2 show the median temperature differences between COSMIC and MLS temperatures obtained from near simultaneous observations in space and time and the corresponding standard deviations, respectively. Here the maximum numbers of simultaneous observations are present in the 50° to 80° and −80° to −50° latitudinal bands, due to the orbital nature of Aura satellite. The median differences are very small and oscillate between −1 and +2 K up to ~ 2 hPa altitude in all latitude regions. At 1 hPa, COSMIC temperatures are less than MLS temperatures by 2–4 K, equal at 0.6–0.7 hPa and above this altitude, the differences are positive and large, and maximise (7–10 K) at 0.3 hPa. Seasonal differences are observed only in high latitudes and high altitudes (< 2 hPa). Standard deviations are less than 2 K from 100 to 20 hPa in low-and mid-latitudes. They increase with altitude and at 1 hPa are less than 5 K over low-latitudes and range from 5–9 K over mid-latitudes. Winter deviations over mid-latitudes are high and summer deviations are similar to those observed

AMTD
6, 6187–6213, 2013

Validation of COSMIC data

U. Das and C. J. Pan

over low-latitudes. Over high-latitudes also, summer deviations are similar to those observed over low- and mid-latitudes while the winter deviations are the highest (> 10 K at 1 hPa).

The oscillatory behavior of the differences between COSMIC and MLS temperatures at altitudes below 1 hPa is very similar to the oscillatory behavior in the observed bias uncertainty of the MLS temperature biases (Livesey et al., 2011). The slightly larger negative difference at 1 hPa and the very high positive difference at 0.3 hPa are also similar to the MLS bias uncertainties. Thus from the comparison of COSMIC temperatures with those from SABER and MLS measurements, we can conclude that COSMIC temperatures are of greater quality, especially due to the reason that the observed differences are most likely produced due to the biases in the retrievals of the latter.

4 Comparison with radiosonde observations

Figure 3 shows the comparison of COSMIC temperature profiles with those observed from radiosondes over Taipei. The top panel shows the radiosonde temperature on 7 August 2011 at 00:00 h UTC and near-simultaneous (within ±5° and ±0.5 h) COSMIC observed temperatures, of which the red profile is the closest in space. This particular day was chosen as there were two COSMIC profiles that we could compare with the radiosonde profile. The differences between COSMIC and radiosonde temperatures at the common altitudes (red and blue profiles) and the differences between the two COSMIC profiles (grey profile) are shown in the top right panel. It can be seen that the two COSMIC profiles differ significantly, especially above 10 hPa. Although near-simultaneous with respect to the radiosonde observations, they are almost 1000 km apart. The differences between COSMIC and radiosonde temperatures are within ±2 K and at the tropopause (∼ 90 hPa) the differences are positive and high. We found 34 such near-simultaneous observations and their differences are shown in the bottom panel of Fig. 3. The grey lines are the individual differences, thick solid black line is the mean of the differences, and the thin solid black lines on either side of the mean

AMTD
6, 6187–6213, 2013
Validation of COSMIC data
U. Das and C. J. Pan

are 1σ deviations. Up to the tropopause, both temperatures match very well. At the tropopause, the COSMIC temperatures are higher than the radiosonde temperatures and the spread is also large with standard deviations of $\sim$3 K. Above the tropopause in the lower stratosphere, the COSMIC temperatures are lower than the radiosonde temperatures by about 1 K and the standard deviations are about 2 K. It can be thus summarized that the COSMIC temperatures match very well with the in situ radiosonde observations over Taipei.

5 Comparison with reanalysis outputs

Figure 4 shows the global seasonal means of COSMIC temperatures and the various reanalysis outputs – NCEP, ERA-Interim, and UKMO, at various pressure levels. At 100 hPa (rows 1 to 4 from bottom), all temperatures are minimum over the tropics during all seasons and maximum in the summer high latitudes. During DJF and JJA, all temperatures look similar, both in variation and magnitude. However, during MAM and SON, COSMIC, NCEP, and ERA temperatures are similar while UKMO temperatures differ significantly, especially at high latitudes. At 10 hPa (rows 5 to 8 from bottom), minimum temperatures are observed over winter high latitudes and maximum temperatures over summer high latitudes. Over tropics the temperatures do not show any significant seasonal variation. At this pressure level also, COSMIC temperatures are similar to NCEP and ERA temperatures, while UKMO temperatures vary significantly. At 1 hPa (rows 3 to 5 from above) also, COSMIC and ERA temperatures match fairly well, while UKMO temperatures differ significantly. Maximum temperatures are observed in summer high latitudes and minimum temperatures in winter high latitudes with tropics showing no significant seasonal variation. And at 0.5 hPa (rows 1 and 2 from above), we only have UKMO temperatures for comparison with COSMIC temperatures which show significant differences again. Maximum COSMIC temperatures are seen over southern high latitudes during SON and minimum temperatures observed during DJF in northern high latitudes.

Global differences between seasonal mean temperatures of COSMIC and the various reanalysis outputs at different pressure levels are shown in Fig. 5. Rows 1 to 3 from below show the temperature differences of COSMIC & NCEP (C-N), COSMIC & ERA (C-E), and COSMIC & UKMO (C-U), respectively, at 100 hPa. Note the non-linearity in the color coding of the figure. Negative departures of NCEP from COSMIC are observed mostly over oceans and positive departures are observed over landmasses and are varying in the range from −2 to 1 K. While no such land-ocean contrast is observed in case of comparison with ERA, the departures are very small ranging from −1 to 1 K. UKMO temperatures are also reasonably well compared with COSMIC temperatures during DJF and JJA with differences ranging from −2 to +2 K. During MAM and SON also, the differences are in the same range over low and mid latitudes; and over high latitudes, large differences greater than ±5 K are observed. Rows 4 to 6 from below show similar temperature differences at 10 hPa. In contrast to that observed at 100 hPa, negative departures of NCEP from COSMIC are observed mostly over landmasses and positive departures over oceans during all seasons and range from −3 to 3 K. COSMIC and ERA temperatures compare very well at this level also during all seasons with differences in the range from −2 to 2 K. And UKMO temperatures show reasonably good comparison with COSMIC temperatures only over low latitudes at this pressure level and the differences range from −3 to 0 K. Over mid and high latitudes, COSMIC and UKMO temperatures differ significantly with differences being greater than ±5 K. COSMIC temperatures are greater in summer and vernal equinox and lower in winter and spring equinox. Rows 2 and 3 from above in Fig. 5 show the temperature differences of COSMIC & ERA (C-E) and COSMIC & UKMO (C-U), respectively, at 1 hPa. Significant differences are observed between COSMIC and ERA with mostly negative departures over low and mid-latitudes ranging from −4 to 0 K, large negative departures of about 8 K over northern high-latitudes during JJA and large positive departures of about 8 K over southern high-latitudes during all seasons except DJF, where the departures are small and about 2 K. Very large differences greater than ±10 K are observed between COSMIC and UKMO at 1 hPa. The situation is the same at 0.5 hPa (Row 1 from above

AMTD
6, 6187–6213, 2013

in Fig. 5), where we only have UKMO temperatures for comparison with COSMIC. The differences are greater than ±10 K.

From these figures we can summarize that COSMIC global seasonal temperatures match extremely well with those of ERA-Interim and very well with NCEP at 100 and 10 hPa and reasonably well with ERA-Interim at 1 hPa. UKMO temperatures differ significantly except during DJF and JJA at 100 hPa.

6 Global mean temperature

Global mean temperatures are obtained by averaging the seasonal means over all latitudes and longitudes from the various satellite observations and the reanalysis outputs and shown in the left panel of Fig. 6. 1σ standard deviations are also shown in the figure by horizontal bars. These bars are slightly shifted up/down along the pressure scale for proper perceptibility. All global means match extremely well and are within the 1σ standard deviations. The differences of the various global means from that of COSMIC are shown in the right panel of Fig. 6. Vertical dotted lines mark the temperature differences at −2, 0, and 2 K to aid the eye. The differences are well within the range from −2 to +2 K up to 1 hPa and are very high above this altitude. The trends observed in these differences are very similar to the earlier comparisons of the various seasonal means/medians.

1. SABER: COSMIC temperature is less than SABER temperature by 2 K at 50 hPa and the difference reduces to zero at 3 hPa with increasing height. At further higher altitudes, the differences are increasingly positive. At 1 hPa COSMIC temperature is higher by 2 K and by almost 6 K at 0.3 hPa.

2. MLS: COSMIC temperatures are higher than MLS temperatures by 0 to 2 K from 50 to 2 hPa and the differences are oscillating in this altitude region. At 1 hPa, COSMIC temperature is smaller by ~ 2 K and larger by ~ 2 K at 0.6 hPa. At 0.3 hPa the difference is as high as 9 K.

AMTD
6, 6187–6213, 2013

3. Reanalysis: Global COSMIC temperatures match extremely well with NCEP global mean and with ERA global mean up to 2 hPa and also with UKMO global mean up to 7 hPa. The differences in these cases are very close to zero. At 1 hPa, COSMIC global mean is less than that of ERA mean by 1 K. Maximum differences are seen in the comparison with UKMO above 7 hPa, where the UKMO mean deviates considerably and also oscillates. Peak differences are 4 K at ~ 1.4 hPa, −3 K at 0.5 hPa and 5 K at 0.2 hPa. Thus UKMO global mean matches with that of COSMIC only up to 7 hPa.

7 Conclusions

We have investigated the COSMIC "atmPrf" temperature data by comparing with other satellite (SABER/TIMED and MLS/Aura) temperature retrievals and reanalysis outputs (NCEP, ERA-Interim and UKMO). This validation study shows that this dataset is of great quality, provides unprecedentedly large number of observations spread uniformly all over the globe and can be used for various investigations of the middle atmosphere. The global coverage of COSMIC is highly uniform compared to other satellites as this is a constellation of six micro satellites. Median temperature differences between COSMIC and SABER in different latitude regions show that the COSMIC temperatures are lower than SABER temperatures by 2–3 K in the lower altitudes (> 5 hPa) and greater by 2–3 K at higher altitudes (1 hPa). From 5 to 1 hPa the differences change from negative to positive. This pattern is very systematic in all latitude regions and during all seasons and probably arises from the biases in the SABER temperature retrievals. Similarly, median differences between COSMIC and MLS temperatures are also very similar to the bias uncertainties in the MLS temperature retrieval. The differences are very small below ~ 2 hPa and oscillate between −1 and +2 K; COSMIC temperatures are lower by 2–4 K at 1 hPa and at ~ 0.3 hPa the COSMIC temperatures are greater by 7–10 K. Comparisons with reanalysis outputs show that COSMIC temperatures match extremely well with ERA-Interim temperatures followed by NCEP temperatures. UKMO

AMTD
6, 6187–6213, 2013

Validation of COSMIC data

U. Das and C. J. Pan

temperatures are either very high or low. From all these comparisons we conclude that COSMIC data can be used with confidence up to 1 hPa, i.e., approximately up to the stratopause (∼ 50 km). Above this altitude there are large deviations from the other satellite observations as well as reanalysis outputs. The importance of these comparisons arises from the facts that SABER and MLS temperatures are from limb radiance measurements and the reanalysis outputs are semi-empirical. This strengthens the credibility of COSMIC data and emphasizes the capability of the GPS RO technique and also the efficiency and need for having not one but a constellation of such satellites for atmospheric sounding.

Earlier the COSMIC data was available only up to 40 km and was reliable only up to ∼ 30 km. This new dataset extends further up to 60 km and is reliable up to ∼ 50 km as the present validation study reveals. Thus, there is a 20 km extension of reliable temperature data in the middle atmosphere that will open up new frontiers to investigate various geophysical processes in the stratosphere and the stratopause region. For example, in Kelvin wave studies using COSMIC "wetPrf" data (Das and Pan, 2013; Pan et al., 2011), conclusive results could not be drawn above 30–35 km due to the large deviations. The new "atmPrf" dataset, providing high quality data, can be used for extending these investigations to high altitudes to obtain better insights in to the understanding of the Kelvin wave propagation. Many other geophysical phenomena in the 100 to 1 hPa region can be better investigated with this dataset.

Acknowledgements. The authors thank S. S. Yang for his help and support. The authors acknowledge the UCAR/COSMIC program, SABER/TIMED and MLS/Aura teams for providing free access to the temperature data, NOAA/OAR/ESRL PSD, Boulder, Colorado, USA, for the NCEP reanalysis data from their Web site at http://www.esrl.noaa.gov/psd/ and UK Meteorological Office (UKMO) for the stratospheric assimilated data through the British Atmospheric Data Centre (BADC). ECMWF ERA-Interim data used in this study have been obtained from the ECMWF data server. The Central Weather Bureau of Taiwan is also acknowledged for providing the Radiosonde data. U. Das and C. J. Pan are supported by the NSC of Taiwan through grant NSC 101-2111-M-008-011.

References

Anthes, R. A., Ector, D., Hunt, D. C., Kuo, Y. H., Rocken, C., Schreiner, W. S., Sokolovskiy, S. V., Syndergaard, S., Wee, T. K., Zeng, Z., Bernhardt, P. A., Dymond, K. F., Chen, Y., Liu, H., Manning, K., Randel, W. J., Trenberth, K. E., Cucurull, L., Healy, S. B., Ho, S. P., McCormick, C., Meehan, T. K., Thompson, D. C., and Yen, N. L.: The COSMIC/FORMOSAT-3 mission: early results, B. Am. Meteorol. Soc., 89, 313–333, 2008. 6189, 6191

Clark, G. Q. and McCoy, J. G.: Measurement of stratospheric temperature, J. Appl. Meteorol., 4, 365–370, 1965. 6189

Das, U. and Pan, C. J.: Strong Kelvin wave activity observed during the westerly phase of QBO – a case study, Ann. Geophys., 31, 581–590, doi:10.5194/angeo-31-581-2013, 2013. 6203

Dee, D. P., Uppala, S. M., Simmons, A. J., Berrisford, P., Poli, P., Kobayashi, S., Andrae, U., Balmaseda, M. A., Balsamo, G., Bauer, P., Bechtold, P., Beljaars, A. C. M., van de Berg, L., Bidlot, J., Bormann, N., Delsol, C., Dragani, R., Fuentes, M., Geer, A. J., Haimberger, L., Healy, S. B., Hersbach, H., Hólm, E. V., Isaksen, L., Kållberg, P., Köhler, M., Matricardi, M., McNally, A. P., Monge-Sanz, B. M., Morcrette, J. J., Park, B. K., Peubey, C., de Rosnay, P., Tavolato, C., Thépaut, J. N., and Vitart, F.: The ERA-Interim reanalysis: configuration and performance of the data assimilation system, Q. J. Roy. Meteorol. Soc., 137, 553–597, 2011. 6194

Dessler, A. E., Burrage, M. D., Grooss, J.-U., Holton, J. R., Lean, J. L., Massie, S. T., Schoeberl, M. R., Douglass, A. R., and Jackman, C. H.: Selected science highlights from the first 5 years of the upper atmosphere research satellite (UARS) program, Rev. Geophys., 36, 183–210, 1998. 6189

Fong, C. J., Yen, N. L., Chu, C. H., Yang, S. K., Shiau, W. T., Huang, C. Y., Chi, S., Chen, S. S., Liou, Y. A., and Kuo, Y. H.: FORMOSAT-3/COSMIC spacecraft constellation system, mission results, and prospect for follow-on mission, Terr. Atmos. Ocean Sci., 20, 1–19, 2009, http://www.ocean-sci.net/20/1/2009/. 6189, 6191

Hauchecorne, A. and Chanin, M.-L.: Density and temperature profiles obtained by lidar between 35 and 70 km, Geophys. Res. Lett., 7, 565–568, doi:10.1029/GL007i008p00565, 1980. 6189

He, W., Ho, S.-P., Chen, H., Zhou, X., Hunt, D., and Kuo, Y.-H.: Assessment of radiosonde temperature measurements in the upper troposphere and lower stratosphere using COSMIC radio occultation data, Geophys. Res. Lett., 36, L17807, doi:10.1029/2009GL038712, 2009. 6190

AMTD
6, 6187–6213, 2013

Validation of COSMIC data

U. Das and C. J. Pan

Kalnay, E., Kanamitsu, M., Kistler, R., Collins, W., Deaven, D., Gandin, L., Iredell, M., Saha, S., White, G., Woollen, J., Zhu, Y., Leetmaa, A., Reynolds, R., Chelliah, M., Ebisuzaki, W., Higgins, W., Janowiak, J., Mo, K. C., Ropelewski, C., Wang, J., Jenne, R., and Joseph, D.: The NCEP/NCAR 40-year reanalysis project, B. Am. Meteorol. Soc., 77, 437–471, 1996. 6194

Kishore, P., Namboothiri, S. P., Jiang, J. H., Sivakumar, V., and Igarashi, K.: Global temperature estimates in the troposphere and stratosphere: a validation study of COSMIC/FORMOSAT-3 measurements, Atmos. Chem. Phys., 9, 897–908, doi:10.5194/acp-9-897-2009, 2009. 6189

Kuo, Y.-H., Wee, T.-K., Sokolovskiy, S., Rocken, C., Schreiner, W., Hunt, D., and Anthes, R.: Inversion and error estimation of GPS radio occultation data, J. Meteorol. Soc. Japan, 82, 507–531, 2004. 6189, 6191

Kuo, Y.-H., Schreiner, W. S., Wang, J., Rossiter, D. L., and Zhang, Y.: Comparison of GPS radio occultation soundings with radiosondes, Geophys. Res. Lett., 32, L05817, doi:10.1029/2004GL021443, 2005. 6189

Kursinski, E. R., Hajj, G. A., Schofield, J. T., Linfield, R. P., and Hardy, K. R.: Observing Earth's atmosphere with radio occultation measurements using the Global Positioning System, J. Geophys. Res., 102, 23429–23465, doi:10.1029/97JD01569, 1997. 6191

Livesey, N. J., Read, W. G., Froidevaux, L., Lambert, A., Manney, G. L., Pumphrey, H. C., Santee, M. L., Schwartz, M. J., Wang, S., Cofeld, R. E., Cuddy, D. T., Fuller, R. A., Jarnot, R. F., Jiang, J. H., Knosp, B. W., Stek, P. C., Wagner, A. P., and Wu, D. L.: Earth Observing System (EOS) Microwave Limb Sounder (MLS) Version 3.3 Level 2 data quality and description document, Tech. rep., Jet Propul. Lab., Pasadena, California, 2011. 6193, 6198

Lorenc, A. C., Ballard, S. P., Bell, R. S., Ingleby, N. B., Andrews, P. L. F., Barker, D. M., Bray, J. R., Clayton, A. M., Dalby, T., Li, D., Payne, T. J., and Saunders, F. W.: The Met. Office global three-dimensional variational data assimilation scheme, Q. J. Roy. Meteorol. Soc., 126, 2991–3012, 2000. 6195

Mertens, C. J., Mlynczak, M. G., López-Puertas, M., Wintersteiner, P. P., Picard, R. H., Winick, J. R., Gordley, L. L., and Russell III, J. M.: Retrieval of mesospheric and lower thermospheric kinetic temperature from measurements of CO_2 15 µm Earth limb emission under non-LTE conditions, Geophys. Res. Lett., 28, 1391–1394, 2001. 6197

Pan, C. J., Das, U., Yang, S. S., Wong, C. J., and Lai, H. C.: Investigation of Kelvin waves in the stratosphere using FORMOSAT-3/COSMIC temperature data, J. Meteorol. Soc. Japan, 89A, 83–96, 2011. 6203

Remsberg, E. E., Marshall, B. T., Garcia-Comas, M., Krueger, D., Lingenfelser, G. S., Martin-Torres, J., Mlynczak, M. G., Russell, J. M., Smith, A. K., Zhao, Y., Brown, C., Gordley, L. L., Lopez-Gonzalez, M. J., Lopez-Puertas, M., She, C. Y., Taylor, M. J., and Thompson, R. E.: Assessment of the quality of the version 1.07 temperature-versus-pressure profiles of the middle atmosphere from TIMED/SABER, J. Geophys. Res., 113, D17101, doi:10.1029/2008JD010013, 2008. 6192, 6197

Rinsland, C. P., Goldman, A., Murcray, F. J., Murcray, D. G., Smith, M. A. H., Seals Jr., R. K., Larsen, J. C., and Rinsland, P. L.: Stratospheric temperature profile from balloon-borne measurements of the 10.4-µm band of CO_2, J. Quant. Spectrosc. Ra., 30, 327–334, doi:10.1016/0022-4073(83)90030-4, 1983. 6189

Schwartz, M. J., Lambert, A., Manney, G. L., Read, W. G., Livesey, N. J., Froidevaux, L., Ao, C. O., Bernath, P. F., Boone, C. D., Cofield, R. E., Daffer, W. H., Drouin, B. J., Fetzer, E. J., Fuller, R. A., Jarnot, R. F., Jiang, J. H., Jiang, Y. B., Knosp, B. W., Krüger, K., Li, J. L. F., Mlynczak, M. G., Pawson, S., Russell, J. M., Santee, M. L., Snyder, W. V., Stek, P. C., Thurstans, R. P., Tompkins, A. M., Wagner, P. A., Walker, K. A., Waters, J. W., and Wu, D. L.: Validation of the Aura Microwave Limb Sounder temperature and geopotential height measurements, J. Geophys. Res., 113, D15S11, doi:10.1029/2007JD008783, 2008. 6193

Swinbank, R. and Great Britian, Meteorological Office: A 3-D Variational Data Assimilation System for the Stratosphere and Troposphere, Numerical Weather Prediction Division, Met Office, Great Britain, 2002. 6195

Waters, J. W., Froidevaux, L., Harwood, R. S., Jarnot, R. F., Pickett, H. M., Read, W. G., Siegel, P. H., Cofield, R. E., Filipiak, M. J., Flower, D. A., Holden, J. R., Lau, G. K., Livesey, N. J., Manney, G. L., Pumphrey, H. C., Santee, M. L., Wu, D. L., Cuddy, D. T., Lay, R. R., Loo, M. S., Perun, V. S., Schwartz, M. J., Stek, P. C., Thurstans, R. P., Boyles, M. A., Chandra, K. M., Chavez, M. C., Chen, G.-S., Chudasama, B. V., Dodge, R., Fuller, R. A., Girard, M. A., Jiang, J. H., Jiang, Y., Knosp, B. W., LaBelle, R. C., Lam, J. C., Lee, K. A., Miller, D., Oswald, J. E., Patel, N. C., Pukala, D. M., Quintero, O., Scaff, D. M., Van Snyder, W., Tope, M. C., Wagner, P. A., and Walch, M. J.: The Earth Observing System Microwave Limb Sounder (EOS MLS) on the Aura satellite, IEEE T. Geosci. Remote, 44, 1075–1092, 2006. 6193

Wickert, J., Reigber, C., Beyerle, G., König, R., Marquardt, C., Schmidt, T., Grunwaldt, L., Galas, R., Meehan, T. K., Melbourne, W. G., and Hocke, K.: Atmosphere sounding by

AMTD

6, 6187–6213, 2013

Validation of COSMIC data

U. Das and C. J. Pan

GPS radio occultation: first results from CHAMP, Geophys. Res. Lett., 28, 3263–3266, doi:10.1029/2001GL013117, 2001. 6189

Wickert, J., Beyerle, G., König, R., Heise, S., Grunwaldt, L., Michalak, G., Reigber, C., and Schmidt, T.: GPS radio occultation with CHAMP and GRACE: a first look at a new and promising satellite configuration for global atmospheric sounding, Ann. Geophys., 23, 653–658, doi:10.5194/angeo-23-653-2005, 2005. 6189

AMTD
6, 6187–6213, 2013

U. Das and C. J. Pan

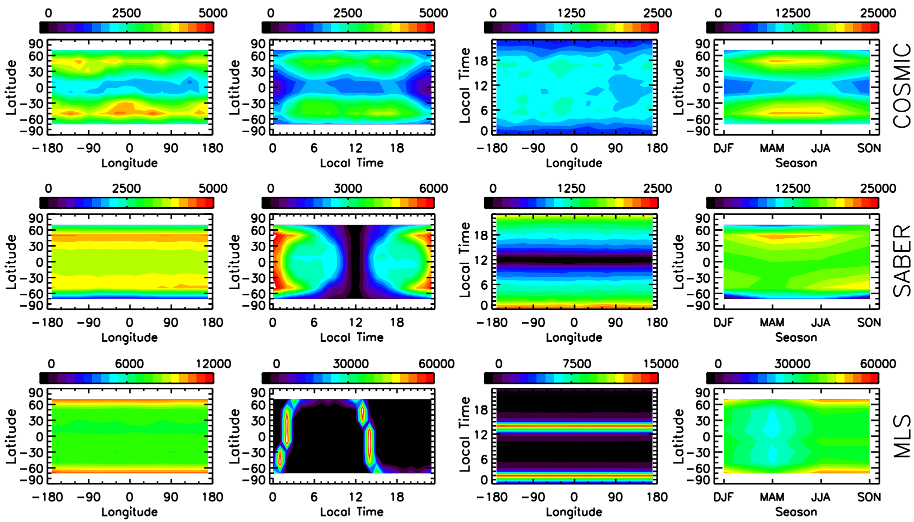

Fig. 1. The global distribution of number of temperature profiles from COSMIC (top row), SABER (middle row) and MLS (bottom row), with respect to space, time and season.

AMTD
6, 6187–6213, 2013

U. Das and C. J. Pan

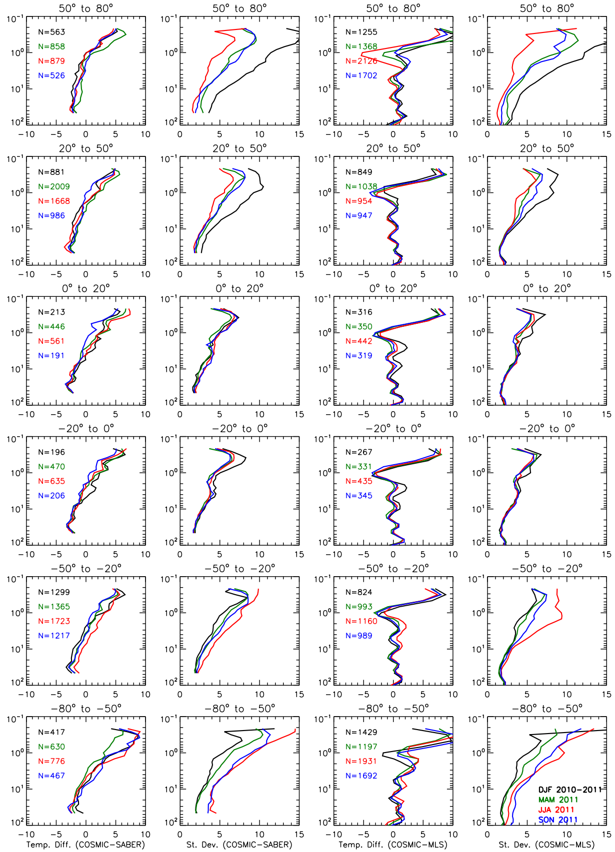

Fig. 2. Seasonal median temperature differences between COSMIC and SABER and COSMIC and MLS temperatures obtained from near simultaneous observations in space and time (columns 1 and 3) and the corresponding standard deviations (columns 2 and 4) in different latitudinal regions (rows) and during different seasons (profile colour).

AMTD
6, 6187–6213, 2013

Validation of COSMIC data

U. Das and C. J. Pan

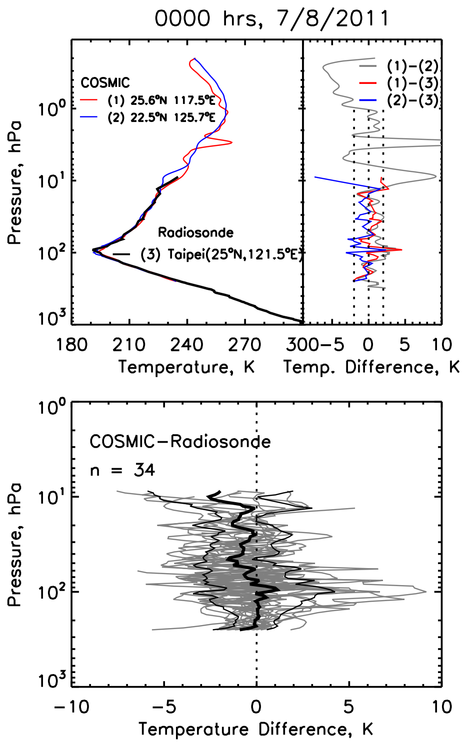

Fig. 3. Top: radiosonde temperature on 7 August 2011 at 00:00 h UTC over Taipei and near-simultaneous (within ±5° and ±0.5 h) COSMIC temperatures. The differences between COSMIC and radiosonde temperatures at the common altitudes (red and blue profiles) and the differences between the two COSMIC profiles (grey profile) are shown in the right panel. Bottom: differences from near-simultaneous observations with the mean difference shown by thick black line and 1σ deviations by thin black lines on either side.

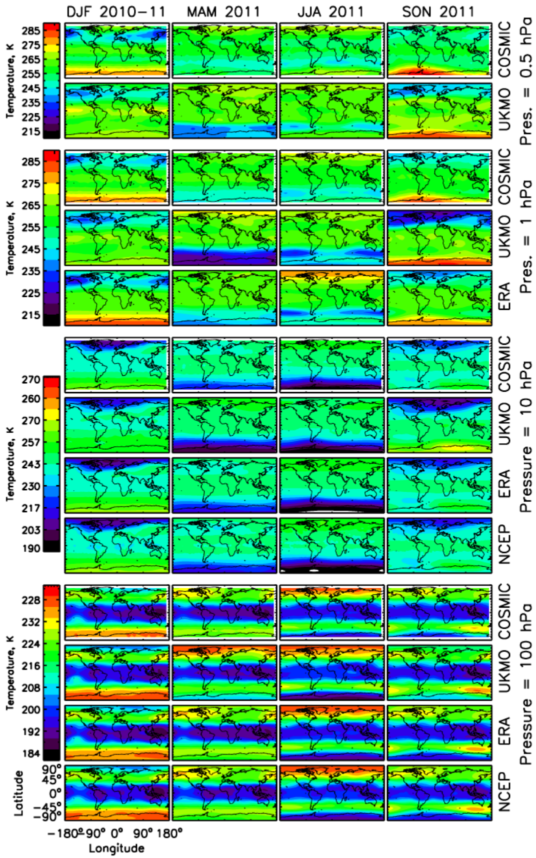

Fig. 4. Global seasonal means of COSMIC temperatures and the various reanalysis outputs – NCEP, ERA-Interim, and UKMO, at the pressure levels 100 hPa (rows 1 to 4 from bottom), 10 hPa (rows 5 to 8 from bottom), 1 hPa (rows 3 to 5 from above) and 0.5 hPa (rows 1 and 2 from above).

AMTD
6, 6187–6213, 2013

Validation of COSMIC data

U. Das and C. J. Pan

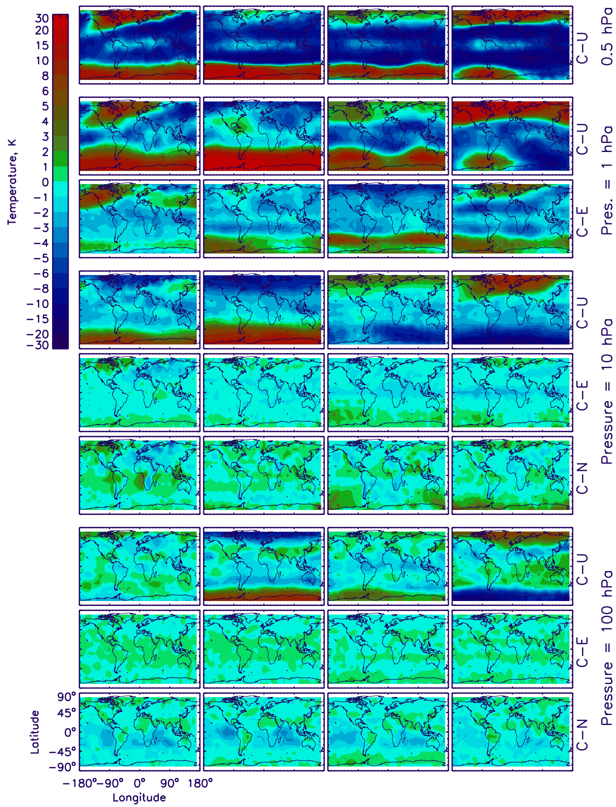

Fig. 5. Differences between the global seasonal means of COSMIC (C) and the reanalysis outputs – NCEP (N), ERA-Interim (E) and UKMO (U) – at 100 hPa (rows 1 to 3 from bottom), 10 hPa (rows 4 to 6 from bottom), 1 hPa (rows 2 and 3 from above) and 0.5 hPa (row 1 from above). Observe the non-linearity in the colour coding.

AMTD

6, 6187–6213, 2013

Validation of COSMIC data

U. Das and C. J. Pan

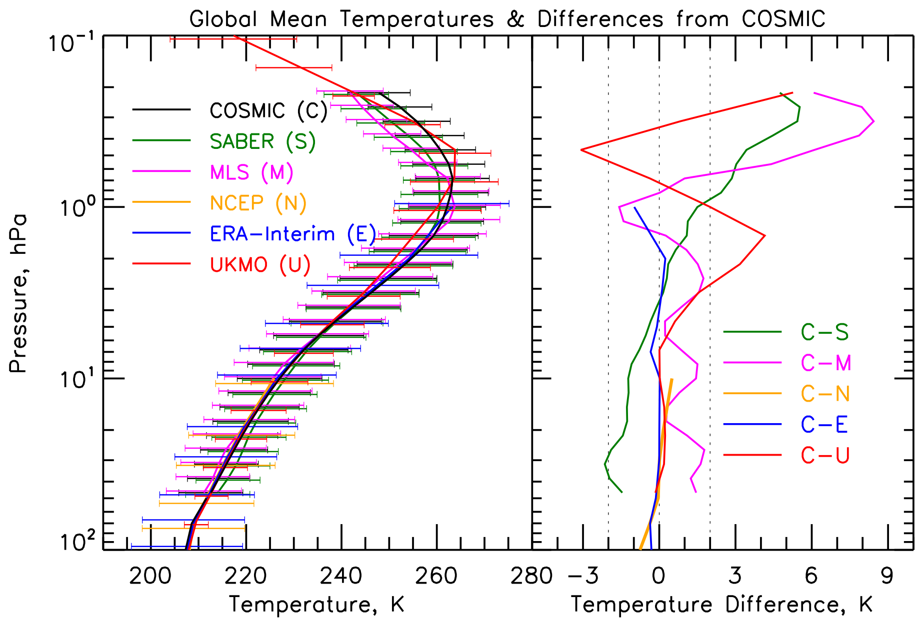

Fig. 6. Right: global mean temperatures from COSMIC (C), SABER (S), MLS (M), NCEP (N), ERA-Interim (E) and UKMO (U). Left: differences from the COSMIC global mean temperature.

AMTD
6, 6187–6213, 2013

Validation of COSMIC data

U. Das and C. J. Pan